

Cosmic reionization after Planck

Sourav Mitra^{1*}, T. Roy Choudhury^{2†} and Andrea Ferrara^{3‡}

¹*University of the Western Cape, Bellville, Cape Town 7535, South Africa*

²*National Centre for Radio Astrophysics, TIFR, Post Bag 3, Ganeshkhind, Pune 411007, India*

³*Scuola Normale Superiore, Piazza dei Cavalieri 7, 56126 Pisa, Italy*

2 March 2024

ABSTRACT

Cosmic reionization holds the key to understand structure formation in the Universe, and can inform us about the properties of the first sources, as their star formation efficiency and escape fraction of ionizing photons. By combining the recent release of Planck electron scattering optical depth data with observations of high-redshift quasar absorption spectra, we obtain strong constraints on viable reionization histories. We show that inclusion of Planck data favors a reionization scenario with a single stellar population. The mean x_{HI} drops from ~ 0.8 at $z = 10.6$ to $\sim 10^{-4}$ at $z = 5.8$ and reionization is completed around $5.8 \lesssim z \lesssim 8.5$ (2σ), thus indicating a significant reduction in contributions to reionization from high redshift sources. We can put independent constraints on the escape fraction f_{esc} of ionizing photons by incorporating the high-redshift galaxy luminosity function data into our analysis. We find a non-evolving f_{esc} of $\sim 10\%$ in the redshift range $z = 6 - 9$.

Key words: dark ages, reionization, first stars – intergalactic medium – cosmology: theory – large-scale structure of Universe.

1 INTRODUCTION

Cosmic reionization is one of the key events in the history of Universe. Most of the available constraints on the epoch of reionization (EoR) come from the observations of the CMB by the Wilkinson Microwave Anisotropy Probe (WMAP) satellite (Komatsu et al. 2011; Hinshaw et al. 2013; Bennett et al. 2013), and from high redshift QSOs (Becker et al. 2001; White et al. 2003; Fan et al. 2006). The recent nine-year WMAP observations provide the value of integrated Thomson scattering optical depth $\tau_{\text{el}} = 0.089 \pm 0.014$ (Hinshaw et al. 2013). This in turn corresponds to an instantaneous reionization taking place at redshift $z_{\text{reion}} = 10.6 \pm 1.1$, indicating a strong need for sources of reionization at $z \gtrsim 10$. However, improved measurements from three-year Planck mission suggest a lower value, $\tau_{\text{el}} = 0.066 \pm 0.012$, (Planck Collaboration et al. 2015) corresponding to $z_{\text{reion}} = 8.8^{+1.2}_{-1.1}$ and therefore cuts down the demand for reionization sources beyond redshift $z = 10$ (Robertson et al. 2015; Bouwens et al. 2015a). The resulting reionization histories seem to explain the observations of Lyman- α emitters at $z \sim 7$ (Mesinger et al. 2015; Choudhury et al. 2014) which were otherwise in tension with the WMAP constraints. Although, these observations of cosmological data analysis are based on the assumption that reionization is a sudden and instantaneous process, recent studies (Barkana & Loeb 2001; Choudhury & Ferrara 2006a,b; Choudhury 2009; Pritchard et al.

2010; Mitra et al. 2011, 2012; Ghara et al. 2015) clearly support a more extended process spanning the redshift range $6 < z < 15$. Several semi-analytical models have been proposed with a combination of different observations to put tighter limits on the reionization redshift and other quantities related to reionization (Choudhury & Ferrara 2005; Wyithe & Loeb 2005; Gallerani et al. 2006; Dijkstra et al. 2007; Samui et al. 2007; Iliev et al. 2008; Mitra et al. 2011; Kulkarni & Choudhury 2011; Mitra et al. 2012; Cai et al. 2014).

Another observation set that could be used to check the consistency of such models is Luminosity Function (LF) of high- z ($6 \lesssim z \lesssim 10$) galaxies (Bouwens & Illingworth 2006; Oesch et al. 2012; Bradley et al. 2012; Oesch et al. 2014; Bowler et al. 2014; McLeod et al. 2014; Bouwens et al. 2015b). This procedure has to deal with the yet poorly understood escape fraction of ionizing photons (f_{esc}). Despite of numerous impressive efforts in both observational and theoretical studies, this quantity, as a function of galaxy mass and redshift, remains largely uncertain (Fernandez & Shull 2011). Available studies generally lead to a broad range and as well as contradictory trends of f_{esc} on redshift. For example, Finkelstein et al. (2012) estimated average f_{esc} to be $\sim 30\%$ in order to get a fully ionized IGM at $z = 6$. Kuhlen & Faucher-Giguère (2012) found a strong redshift evolution of escape fraction increasing from $\sim 4\%$ at $z = 4$ to unity at higher redshifts in order to simultaneously satisfy reionization and lower redshift Lyman- α forest constraints. Based on a robust statistical analysis on full CMB spectrum and quasar data and using the observations of high- z galaxy LFs, we (Mitra et al. 2013) derived that mean value of f_{esc} is moderately increasing from 7% at $z = 6$

* E-mail: hisourav@gmail.com

† E-mail: tirth@ncra.tifr.res.in

‡ E-mail: andrea.ferrara@sns.it

to 18% at $z = 8$. This increasing behavior of f_{esc} on redshift is somewhat similar to that obtained or assumed in Inoue et al. (2006); Razoumov & Sommer-Larsen (2010); Haardt & Madau (2011, 2012); Ferrara & Loeb (2013); Finlator et al. (2015). More recently, using a high-resolution cosmological zoom-in simulation of galaxy formation, Ma et al. (2015) found a considerably lower ($< 5\%$; much less than required by reionization models) and a non-evolving escape fraction. This unchanging trend of f_{esc} is as well consistent with many other earlier results (Gnedin 2008; Yajima et al. 2011). A decreasing tendency of escape fraction with redshift has also been reported in the literature (Wood & Loeb 2000; Kimm & Cen 2014).

For all these reasons, here we revise our reionization models (Mitra et al. 2013) in the light of recently available Planck data and improved measurements of high- z LFs¹.

2 DATA-CONSTRAINED REIONIZATION MODEL

Let us first summarize the main features of the semi-analytical model for inhomogeneous reionization used in this analysis, which is based on Choudhury & Ferrara (2005) and Choudhury & Ferrara (2006b). The model tracks the ionization and thermal evolution of all hydrogen and helium regions separately and self-consistently by adopting a *lognormal* probability distribution² at low densities, changing to a *power-law* at high densities (Choudhury & Ferrara 2005). The model considers the inhomogeneities in the IGM according to the description given by MHR (Miralda-Escudé et al. 2000), in which once all the low-density regions are ionized, reionization is said to be complete (see Choudhury 2009).

The sources of reionization are assumed to be stars (metal-free PopIII and normal PopII) and quasars. The contribution of quasars are incorporated here based on their observed luminosity function at $z < 6$ (Hopkins et al. 2007) and they have insignificant effects on IGM at higher redshifts (but also see Giallongo et al. 2015; Madau & Haardt 2015). Furthermore, the model calculates the suppression of star formation in low-mass haloes (*radiative feedback*) through a Jeans mass prescription, which is computed self-consistently from the evolution of the thermal properties of IGM through the minimum circular velocity of haloes that are able to cool (Choudhury & Ferrara 2005; also comparable to the simulations by Okamoto et al. 2008; Sobacchi & Mesinger 2013). Our model also accounts for the *chemical feedback* (PopIII \rightarrow PopII transition) using merger-tree based genetic approach (Schneider et al. 2006). The model computes the production rate of ionizing photons in the IGM as

$$\dot{n}_{\text{ph}}(z) = n_b N_{\text{ion}} \frac{df_{\text{coll}}}{dt} \quad (1)$$

where, f_{coll} is the collapsed fraction of dark matter halo, n_b is the total baryonic number density in the IGM and N_{ion} , possibly a function of halo mass and redshift, is the number of photons entering the IGM per baryon in stars. However, throughout this work

we assume N_{ion} to be independent of halo mass. This quantity can be written as $N_{\text{ion}} = \epsilon_* f_{\text{esc}} N_\gamma$, where ϵ_* is the star formation efficiency, and N_γ is the specific number of photons emitted per baryon in stars (Mitra et al. 2013):

2.1 MCMC-PCA constraints from Planck data

From the above model, we obtain the redshift evolution of $N_{\text{ion}}(z)$ and other quantities by performing a detailed likelihood estimation using the Principal Component Analysis (PCA), following Mitra et al. (2011, 2012). We assume N_{ion} as an arbitrary function of z and decompose it into its principal components by constructing the Fisher matrix from a fiducial model for N_{ion} using three different datasets: (i) measurements of photoionization rates Γ_{PI} in $2.4 \leq z \leq 6$ from Bolton & Haehnelt (2007) and Becker & Bolton (2013)³; (ii) redshift evolution of Lyman-limit systems (LLS), dN_{LL}/dz over a wide redshift range ($0.36 < z < 6$) by Songaila & Cowie (2010)⁴; (iii) Thomson scattering optical depth τ_{el} using recent Planck data (Planck Collaboration et al. 2015). We further impose fairly model-independent constraints on neutral hydrogen fraction at $z \sim 5 - 6$ from McGreer et al. (2015) as a prior to our model. We choose the fiducial model to be constant (no redshift dependence) as it matches the above-mentioned data points quite accurately. When computing the ionizing radiation properties, we include only a single stellar population (PopII) and neglect the contributions from PopIII sources (thus no *chemical feedback* in the model) since such effects will be indirectly included in the evolution of N_{ion} itself.

We then take the first 2 – 7 PCA modes (eigen-modes of the Fisher matrix), having the largest eigenvalues or smallest uncertainties, which satisfy a model-independent Akaike information criteria (AIC; Liddle 2007) and finally perform the Markov Chain Monte Carlo (MCMC) analysis⁵ using those modes; for details, see Mitra et al. (2011, 2012). As the Planck collaboration has not published low- ℓ polarization data, we include only Planck optical depth data in the analysis. However, if one may wish to include the full CMB spectra into the analysis, one should also consider variations in σ_8 and n_s to avoid their possible degeneracies with the reionization model parameters (Pandolfi et al. 2011; Mitra et al. 2012).

The MCMC constraints on the model are shown in Fig. 1. The fiducial model is well inside the shaded regions for all redshift range. One can see that, overall our model predictions match the observed data points quite reasonably. We find that, all the quantities are tightly constrained at $z \lesssim 6$. This is expected as most of the observational information considered in this work exists only at those redshifts. On the other hand, a wide range of histories at $z > 6$ is still permitted by the data. The 2- σ confidence limits (C.L.) start to decrease at redshift $z \gtrsim 13$ since the components of

¹ Throughout this Letter, we assume a flat Universe with Planck cosmological parameters: $\Omega_m = 0.3089$, $\Omega_\Lambda = 1 - \Omega_m$, $\Omega_b h^2 = 0.02230$, $h = 0.6774$, $\sigma_8 = 0.8159$, $n_s = 0.9667$ and $Y_{\text{P}} = 0.2453$ (Planck Collaboration et al. 2015).

² Another commonly employed form of the probability density function (PDF) is an updated version of Miralda-Escudé et al. (2000) fit (Pawlik et al. 2009). However we checked that, the differences in these two PDFs are much smaller than the errors in the data considered here and thus the constraints are unlikely to be affected.

³ The Γ_{PI} measurements of Bolton & Haehnelt (2007) and Becker & Bolton (2013) somewhat depend on their choice of fiducial parameter set. They have provided scaling relations to convert these measurements to any other choice of parameters. While comparing with our models, we have applied appropriate scaling to those for every parameter set considered. The Γ_{PI} data points with errorbars in Fig. 1 reflect the scaled measurements.

⁴ The reason for choosing Songaila & Cowie (2010) datasets over more recent measurements on mean free path of ionizing photons by Worseck et al. (2014) is that the former data covers a wider redshift range, thus helping us to get tighter constraints on reionization parameters.

⁵ All cosmological parameters are fixed at their best-fit Planck value.

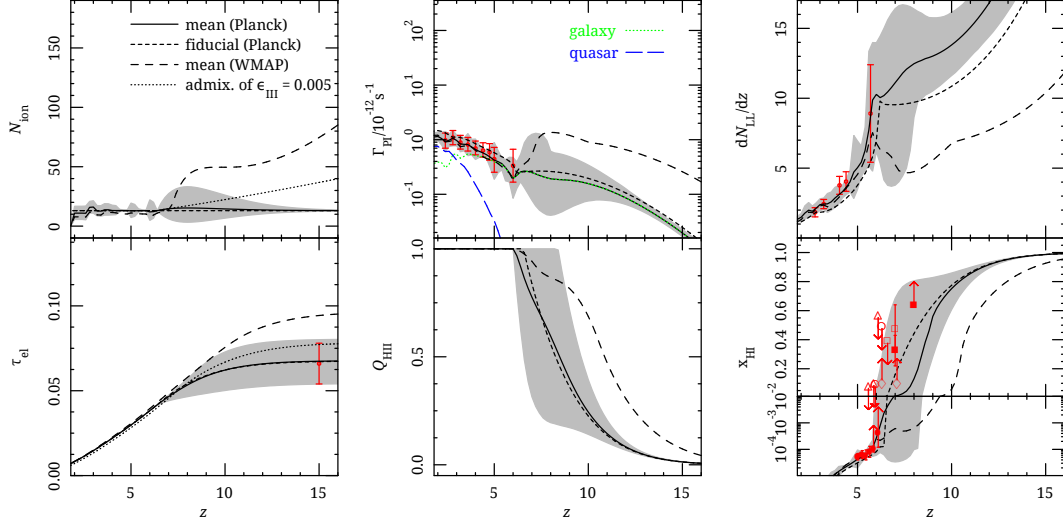


Figure 1. MCMC results: The mean value (solid lines) and its 2- σ limits (shaded regions) for various quantities related to reionization obtained from our current analysis with Planck data. The fiducial model (short-dashed lines) and the model constrained using WMAP9 τ_{el} data (long-dashed lines) also shown for comparison. The red points with errorbars that we have used to constrain the model are taken from the observations of photoionization rates Γ_{PI} (Bolton & Haehnelt 2007; Becker & Bolton 2013; *top-middle* panel), The redshift distribution of LLS dN_{LL}/dz (Songaila & Cowie 2010; *top-right* panel) and the recent measurements of electron scattering optical depth τ_{el} from Planck mission (Planck Collaboration et al. 2015; *bottom-left* panel). We also show the observational limits on neutral hydrogen fraction $x_{\text{HI}}(z)$ (*bottom-right* panel) from various measurements by Fan et al. (2006) (filled circle), McGreer et al. (2015) (open triangle), Totani et al. (2006); Chornock et al. (2013) (open circle), Bolton et al. (2011); Schroeder et al. (2013) (open diamond), Ota et al. (2008); Ouchi et al. (2010) (open square), Schenker et al. (2014) (filled square).

the Fisher matrix are zero and there is no significant information from the PCA modes beyond this point.

For comparison, we also show the model constrained by the WMAP9 $\tau_{\text{el}} = 0.089 \pm 0.014$ value and corresponding cosmological parameters (Hinshaw et al. 2013). The mean evolution of all the quantities for this model is almost identical to the Planck one at $z \lesssim 6$; at earlier epochs they start to differ, as expected from the different e.s. optical depth. However, the mean model for WMAP9 lies within Planck’s 2- σ limits only up to $z \lesssim 7$ or 8. We have further shown a typical admixture of PopIII contributions with $\epsilon_{\text{PopIII}} = 0.005$ ($\epsilon \equiv \epsilon_* f_{\text{esc}}$) to the N_{ion} (dotted black lines), which is the maximum limit that can be allowed by the Planck τ_{el} data. Whereas for the best-fit WMAP9 model, we get $\epsilon_{\text{PopIII}} = 0.014$. The mean evolution of $N_{\text{ion}}(z)$ for Planck closely follows the fiducial model, suggesting that an non-evolving N_{ion} is well-permitted by the current data. This is one of the key results from this work and deserves some more insight.

Unlike the WMAP9 model, the smaller value of τ_{el} from Planck essentially releases the need for high-redshift ionizing sources and allows the reionization to be completed from only a single stellar population (PopII). The mean evolution of photoionization rates Γ_{PI} shows a mild increase at $z > 6$, whereas the WMAP model shows a relatively higher value of Γ_{PI} at early epochs as it still allows the contributions coming from PopIII stars, which are able to produce large number of ionizing photons. A similar trend is also found in the evolution of LLSs. Thus the future observations on LLS around these epochs may able to further discriminate between these two models. In the Γ_{PI} plot, we also show the relative contributions from quasars and galaxies at different redshifts for the mean model by long-dashed (blue) and dotted (green) lines respectively. From the evolution of volume filling factor Q_{HII} for HII regions, one can see that reionization is almost completed ($Q_{\text{HII}} \sim 1$) around $5.8 \lesssim z \lesssim 8.5$ (2- σ limits) for Planck model. The mean ionized fraction evolves

rapidly in $5.8 \lesssim z \lesssim 10.6$, in good agreement with other recent works (George et al. 2015; Robertson et al. 2015), whereas the mean WMAP model favors a relatively gradual or extended reionization (spanning $5.8 \lesssim z \lesssim 13$). This is reflected in the evolution of the neutral hydrogen fraction x_{HI} : the mean value for Planck model goes from $x_{\text{HI}} \sim 0.8$ to $x_{\text{HI}} \sim 10^{-4}$ between $z = 10.6$ ($z = 13$ for WMAP model) and $z = 5.8$. Overall our model prediction for $x_{\text{HI}}(z)$ is consistent with various observational limits (see the caption in the Fig. 1 for references).

3 UV LUMINOSITY FUNCTION

From the above data-constrained reionization models, we now derive the high- z LFs, following Mitra et al. 2013. The luminosity at 1500 Å of a galaxy with mass M and age Δt ($= t_z - t_{z'}$; time elapsed between the redshift of formation z' and redshift of observation z) can be written as (Samui et al. 2007; Kulkarni & Choudhury 2011):

$$L_{1500}(M, \Delta t) = \epsilon_* \left(\frac{\Omega_b}{\Omega_m} \right) M l_{1500}(\Delta t) \quad (2)$$

where, ϵ_* is the star-forming efficiency of PopII stars only as we will restrict ourselves to a single stellar population throughout this analysis. The template specific luminosity l_{1500} is computed from stellar population synthesis model of Bruzual & Charlot (2003) for PopII stars having different metallicities in the range $Z = 0.0001 - 0.05$. Here we have incorporated the mass-metallicity relation given by Dayal et al. (2009) and Dayal et al. (2010) and take the appropriate model with that metallicity. The luminosity is then converted to standard absolute AB magnitude system (Oke & Gunn 1983; Kulkarni & Choudhury 2011), and finally we obtain the LF,

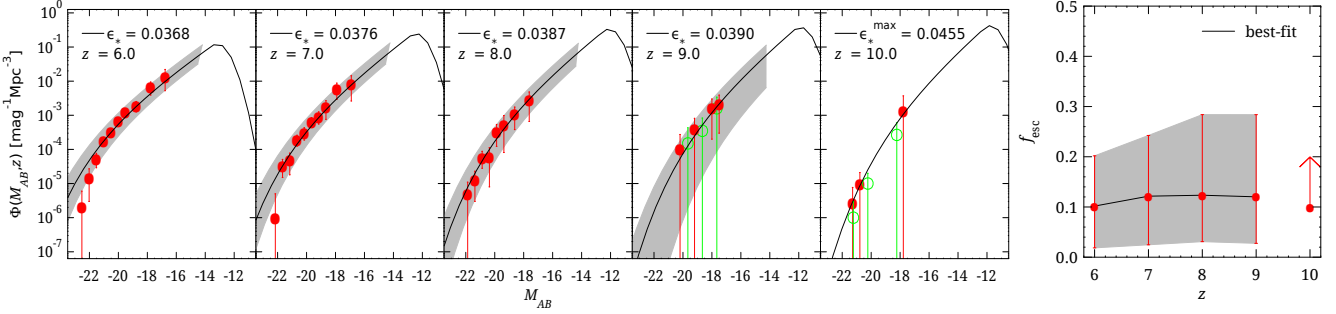


Figure 2. *Left panels:* Evolution of luminosity function from our model for best-fit ϵ_* (black curve) and $2\text{-}\sigma$ limits (shaded region) at $z = 6 - 10$. Data (red) points with $2\text{-}\sigma$ errors are: Bouwens et al. (2015b) (for $z = 6, 7, 8$), combined datasets from McLure et al. (2013) and McLeod et al. (2014) for $z = 9$ and improved data from Oesch et al. (2014) for $z = 10$. For completeness, we also show data from Oesch et al. (2013) for $z = 9$ and Bouwens et al. (2015b) for $z = 10$ (not included in our analysis, open green points). *Right panel:* Redshift evolution of the escape fraction f_{esc} with $2\text{-}\sigma$ errors. The $z = 10$ point shows the lower limit on f_{esc} at that redshift.

$\Phi(M_{AB}, z)$, from

$$\Phi(M_{AB}, z) = \frac{dn}{dM_{AB}} = \frac{dn}{dL_{1500}} \frac{dL_{1500}}{dM_{AB}} \quad (3)$$

where dn/dL_{1500} is the comoving number of objects having luminosity within $[L_{1500}, L_{1500} + dL_{1500}]$ at a redshift z . This quantity can be calculated from the formation rate of haloes using our reionization model (Choudhury & Ferrara 2007).

Now, we vary ϵ_* in eq. 2 as a free parameter and match the observed LFs with our model predictions computed using eq. 3. In Fig. 2 (*left panels*), we show our results for the best-fit ϵ_* with 95% C.L. for redshifts $z = 6 - 10$. As the observations at $z = 10$ are still scant, we are able to determine only an upper limit of ϵ_* . The best-fit ϵ_* remains almost constant ($\sim 4\%$) for all redshift range. The number of galaxies start to decrease at fainter magnitudes producing a “knee”-like shape in the LFs which shifts towards the brighter ends at lower redshifts ($M_{AB} \sim -12$ at $z = 10$ to $M_{AB} \sim -14$ at $z = 6$). This is due to the radiative feedback implemented in our model where the star formation becomes suppressed.

Overall, the match between data and model predictions is quite impressive for all redshifts considered here. The uncertainties (shaded regions) are larger at high- z and at the bright end of LFs. For lower redshifts ($z \leq 7$), although our model can match the fainter end of the LF accurately, it slightly over-predicts the bright end. This general tendency has already been addressed in several recent works (Cai et al. 2014; Dayal et al. 2014; Bowler et al. 2014 and the references therein). In particular, Cai et al. (2014) argued that it can be resolved by taking the dust obscuration into account, which we are neglecting here. As the dust extinction was insignificant at earlier times, we are getting a good match for the brighter end at $z > 7$. Alternatively, the surveyed volumes might be too small to catch the brightest, rare objects (for a discussion, see Bowler et al. 2014; Dayal et al. 2014). However, it is still unclear whether this discrepancy arises from neglecting dust or halo mass quenching (Peng et al. 2010), or it is due to a mass-dependent ϵ_* . Thus it would be interesting to take those effects in our model which we prefer to leave for future work.

3.1 Escape fraction evolution

As a final step, having fixed ϵ_* for different redshifts, we can derive limits for f_{esc} using the reionization constraints on the evolution of N_{ion} (Sec. 2.1) with $N_\gamma = 3200$ as appropriate for the PopII Salpeter IMF assumed here. The uncertainties in f_{esc} can

Redshift	best-fit ϵ_* [$2\text{-}\sigma$ limits]	best-fit f_{esc} [$2\text{-}\sigma$ limits]
$z = 6$	0.0368 [0.0189, 0.0743]	0.1018 [0.0186, 0.2018]
$z = 7$	0.0376 [0.0194, 0.0773]	0.1215 [0.0247, 0.2424]
$z = 8$	0.0387 [0.0170, 0.0764]	0.1234 [0.0309, 0.2839]
$z = 9$	0.0390 [0.0050, 0.0785]	0.1202 [0.0276, 0.2838]
$z = 10$	< 0.0455	> 0.0996

Table 1. Best-fit values and $2\text{-}\sigma$ limits of star-forming efficiency ϵ_* and the escape fraction f_{esc} obtained from the LF matching at different redshifts $z = 6 - 10$. At $z = 10$, we only get an upper limit of ϵ_* and a corresponding lower limit of f_{esc} .

also be calculated using the quadrature method (Mitra et al. 2013). We show our resulting f_{esc} in Table 1 and the *right panel* of Fig. 2. We find almost non-evolving (constant) f_{esc} of $\sim 10\%$ (best-fit) in the redshift range $z = 6 - 9$. For $z = 10$, we get a lower limit of 10% which is a very strong constraint given the uncertainties present in high- z observations.

4 CONCLUSIONS

Over the past few years, several numerical and analytical approaches have tried to constrain reionization scenarios by using CMB WMAP observations and QSOs. In particular, in our earlier works (Mitra et al. 2011, 2012), we proposed a detailed semi-analytical modeling of hydrogen reionization using the observations for photoionization rates, redshift evolution of LLS and CMB and succeeded to produce a good match with a variety of other relevant datasets. We further tested the model against the observations of luminosity functions from high-redshift galaxies (Mitra et al. 2013). In this Letter, we extend those works by taking the recently published τ_{el} data from Planck Collaboration et al. (2015) and various new results from the observations of galaxy LFs at $6 \leq z \leq 10$.

- We find that, contrary to WMAP data, a constant/non-evolving N_{ion} is now allowed by the Planck data. This immediately tells us that, reionization with a single stellar population (PopII) or non-evolving IMF is possible, i.e. the impact of PopIII stars on reionization (Paardekooper et al. 2013) is likely to be negligible.

- According to Planck data, reionization proceeds quickly from $z \approx 10.6$ to $z \approx 5.8$ as the mean x_{HI} drops from 0.8 to 10^{-4} within these epochs. We find that reionization is almost completed around $5.8 \lesssim z \lesssim 8.5$ ($2\text{-}\sigma$ C.L.). However, the model with WMAP data seems to favor an extended reionization starting as

early as $z \approx 13$. Thus, the inclusion of Planck data in turn indicates that most of the reionization activity occurs at $z \lesssim 10$ (Robertson et al. 2015; Bouwens et al. 2015a).

- From the match between the observed high-redshift LFs and our model predictions, we find that the best-fit values for both ϵ_* and f_{esc} remains somewhat constant with redshifts: ϵ_* at $\sim 4\%$ and $f_{\text{esc}} \sim 10\%$ for $z = 6 - 9$ (Gnedin 2008; Yajima et al. 2011; Ma et al. 2015). We have also obtained the tightest constraint available to our knowledge on f_{esc} ($> 10\%$) at $z = 10$.

Although we have focused on high-redshift LFs, one can apply the same method for the evolution in lower redshift range $3 \leq z \leq 5$. As the dust extinction becomes significant at those redshifts, one has to take that into account. Moreover, the addition of dust and/or a mass-dependent ϵ_* may resolve the problem of overproducing the brighter end of LFs, as stated earlier. We defer these issues to future work. Also, the inclusion of *full* CMB datasets from Planck into our analysis can be helpful for ruling out some of the current reionization scenarios. Unfortunately, the recent Planck data release does not include the polarization data in their likelihood; instead, they rely on the WMAP polarization likelihood at low multipoles (Planck Collaboration et al. 2015). As most of the constraints at $z > 6$ related to reionization models come from polarization data (Mitra et al. 2012), we postpone such analysis to the next Planck data release.

REFERENCES

- Barkana R., Loeb A., 2001, *Phys. Rep.*, 349, 125
- Becker G. D., Bolton J. S., 2013, *MNRAS*, 436, 1023
- Becker R. H., et al., 2001, *Astron.J.*, 122, 2850
- Bennett C. L., et al., 2013, *ApJS*, 208, 20
- Bolton J. S., et al., 2011, *MNRAS*, 416, L70
- Bolton J. S., Haehnelt M. G., 2007, *MNRAS*, 382, 325
- Bouwens R., Illingworth G., 2006, *New Astronomy Reviews*, 50, 152
- Bouwens R. J., et al., 2015a, arXiv:1503.08228
- Bouwens R. J., et al., 2015b, *ApJ*, 803, 34
- Bowler R. A. A., et al., 2014, arXiv:1411.2976
- Bradley L. D., et al., 2012, *ApJ*, 760, 108
- Bruzual G., Charlot S., 2003, *MNRAS*, 344, 1000
- Cai Z.-Y., Lapi A., Bressan A., De Zotti G., Negrello M., Danese L., 2014, *ApJ*, 785, 65
- Chornock R., et al., 2013, *ApJ*, 774, 26
- Choudhury T. R., 2009, *Current Science*, 97, 841
- Choudhury T. R., Ferrara A., 2005, *MNRAS*, 361, 577
- Choudhury T. R., Ferrara A., 2006a, arXiv:astro-ph/0603149
- Choudhury T. R., Ferrara A., 2006b, *MNRAS*, 371, L55
- Choudhury T. R., Ferrara A., 2007, *MNRAS*, 380, L6
- Choudhury T. R., Puchwein E., Haehnelt M. G., Bolton J. S., 2014, arXiv:1412.4790
- Dayal P., Ferrara A., Dunlop J. S., Pacucci F., 2014, *MNRAS*, 445, 2545
- Dayal P., Ferrara A., Saro A., 2010, *MNRAS*, 402, 1449
- Dayal P., Ferrara A., Saro A., Salvaterra R., Borgani S., Tornatore L., 2009, *MNRAS*, 400, 2000
- Dijkstra M., Wyithe J. S. B., Haiman Z., 2007, *MNRAS*, 379, 253
- Fan X., et al., 2006, *AJ*, 132, 117
- Fernandez E. R., Shull J. M., 2011, *ApJ*, 731, 20
- Ferrara A., Loeb A., 2013, *MNRAS*, 431, 2826
- Finkelstein S. L., et al., 2012, *ApJ*, 758, 93
- Finlator K., Thompson R., Huang S., Davé R., Zackrisson E., Oppenheimer B. D., 2015, *MNRAS*, 447, 2526
- Gallerani S., Choudhury T. R., Ferrara A., 2006, *MNRAS*, 370, 1401
- George E. M., et al., 2015, *ApJ*, 799, 177
- Ghara R., Datta K. K., Choudhury T. R., 2015, arXiv:1504.05601
- Giallongo E., et al., 2015, *A&A*, 578, A83
- Gnedin N. Y., 2008, *ApJL*, 673, L1
- Haardt F., Madau P., 2011, arXiv:1103.5226
- Haardt F., Madau P., 2012, *ApJ*, 746, 125
- Hinshaw G., et al., 2013, *ApJS*, 208, 19
- Hopkins P. F., Richards G. T., Hernquist L., 2007, *ApJ*, 654, 731
- Iliev I. T., Shapiro P. R., McDonald P., Mellema G., Pen U.-L., 2008, *MNRAS*, 391, 63
- Inoue A. K., Iwata I., Deharveng J.-M., 2006, *MNRAS*, 371, L1
- Kimm T., Cen R., 2014, *ApJ*, 788, 121
- Komatsu E., et al., 2011, *Astrophys.J.Suppl.*, 192, 18
- Kuhlen M., Faucher-Giguère C.-A., 2012, *MNRAS*, 423, 862
- Kulkarni G., Choudhury T. R., 2011, *MNRAS*, 412, 2781
- Liddle A. R., 2007, *MNRAS*, 377, L74
- Ma X., Kasen D., Hopkins P. F., Faucher-Giguère C.-A., Quataert E., Keres D., Murray N., 2015, arXiv:1503.07880
- Madau P., Haardt F., 2015, arXiv:1507.07678
- McGreer I. D., Mesinger A., D’Odorico V., 2015, *MNRAS*, 447, 499
- McLeod D. J., McLure R. J., Dunlop J. S., Robertson B. E., Ellis R. S., Targett T. T., 2014, arXiv:1412.1472
- McLure R. J., et al., 2013, *MNRAS*, 432, 2696
- Mesinger A., Aykutalp A., Vanzella E., Pentericci L., Ferrara A., Dijkstra M., 2015, *MNRAS*, 446, 566
- Miralda-Escudé J., Haehnelt M., Rees M. J., 2000, *ApJ*, 530, 1
- Mitra S., Choudhury T. R., Ferrara A., 2011, *MNRAS*, 413, 1569
- Mitra S., Choudhury T. R., Ferrara A., 2012, *MNRAS*, 419, 1480
- Mitra S., Ferrara A., Choudhury T. R., 2013, *MNRAS*, 428, L1
- Oesch P. A., et al., 2012, *ApJ*, 745, 110
- Oesch P. A., et al., 2013, *ApJ*, 773, 75
- Oesch P. A., et al., 2014, *ApJ*, 786, 108
- Okamoto T., Gao L., Theuns T., 2008, *MNRAS*, 390, 920
- Oke J. B., Gunn J. E., 1983, *ApJ*, 266, 713
- Ota K., et al., 2008, *ApJ*, 677, 12
- Ouchi M., et al., 2010, *ApJ*, 723, 869
- Paardekooper J.-P., Khochfar S., Dalla Vecchia C., 2013, *MNRAS*, 429, L94
- Pandolfi S., Ferrara A., Choudhury T. R., Melchiorri A., Mitra S., 2011, *Phys. Rev. D*, 84, 123522
- Pawlik A. H., Schaye J., van Scherpenzeel E., 2009, *MNRAS*, 394, 1812
- Peng Y.-j., et al., 2010, *ApJ*, 721, 193
- Planck Collaboration et al., 2015, arXiv:1502.01589
- Pritchard J. R., Loeb A., Wyithe J. S. B., 2010, *MNRAS*, 408, 57
- Razoumov A. O., Sommer-Larsen J., 2010, *ApJ*, 710, 1239
- Robertson B. E., Ellis R. S., Furlanetto S. R., Dunlop J. S., 2015, *ApJL*, 802, L19
- Samui S., Srianand R., Subramanian K., 2007, *MNRAS*, 377, 285
- Schenker M. A., Ellis R. S., Konidaris N. P., Stark D. P., 2014, *ApJ*, 795, 20
- Schneider R., Salvaterra R., Ferrara A., Ciardi B., 2006, *MNRAS*, 369, 825
- Schroeder J., Mesinger A., Haiman Z., 2013, *MNRAS*, 428, 3058
- Sobacchi E., Mesinger A., 2013, *MNRAS*, 432, 3340
- Songaila A., Cowie L. L., 2010, *ApJ*, 721, 1448
- Totani T., et al., 2006, *Pub. Astron. Soc. Japan*, 58, 485

6 *Mitra, Choudhury & Ferrara*

White R. L., Becker R. H., Fan X., Strauss M. A., 2003, *AJ*, 126,
1

Wood K., Loeb A., 2000, *ApJ*, 545, 86

Worseck G., et al., 2014, *MNRAS*, 445, 1745

Wyithe J. S. B., Loeb A., 2005, *ApJ*, 625, 1

Yajima H., Choi J.-H., Nagamine K., 2011, *MNRAS*, 412, 411